for their financial support (project acronyms: OPTIMISE, CREATE/CONFOCAL, and GRAPPAS).

REFERENCES

1. http://www.ticra.com/.
2. http://www.mician.com.
3. Y. Chen, R. Mittra, and P. Harms, Finite-difference time-domain algorithm for solving Maxwell's equations in rotationally symmetric geometries, IEEE Trans Microwave Theory Tech 44 (1996), 832–839.
4. A. Rolland, M. Ettore, M. Drissi, L. Le Coq, and R. Sauleau, Optimization of reduced-size smooth-walled conical horns using BoR-FDTD and genetic algorithm, IEEE Trans Antennas Propag 58 (2010), 3094–3100.
5. M. Celuch and W.K. Gwarek, Industrial design of axisymmetrical devices using a customized solver from RF to optical frequency bands, IEEE Microwave Mag 9 (2008), 150–159.
6. A. Rolland, M. Ettore, A.V. Boriskin, L. Le Coq, and R. Sauleau, Axisymmetric resonant lens antenna with improved directivity in Ka-band, IEEE Antennas Wireless Propag Lett 10 (2011), 37–40.
7. Z. Yang, Y. Chen, W. Yu, and R. Mittra, Hybrid FDTD/AutoCAD method for the analysis of BoR horns and reflectors, Microwave Opt Technol Lett 37 (2003), 236–243.
8. M.S. Tong, R. Sauleau, A. Rolland, and T.G. Chang, Analysis of electromagnetic band-gap waveguide structures using body-of-revolution finite-difference time-domain method, Microwave Opt Technol Lett 49 (2007), 2201–2206.
9. A. Taflove and S.C. Hagness, Computational electrodynamics: The finite-difference time-domain method, 2nd ed., Artech House, Norwood, MA, 2000.
10. C. Bruns, P. Leuchtmann, and R. Vahldieck, Comprehensive analysis and simulation of a 1-18 GHz broadband parabolic reflector horn antenna system, IEEE Trans Antennas Propag 51 (2003), 1418–1423.
11. M. Arrebola, L. Haro, and J. Encinar, Analysis of dual-reflector antennas with a reflectarray as subreflector, IEEE Antennas Propag Mag 50 (2008), 1418–1423.
12. R. Pascaud, R. Gillard, R. Loison, J. Wiart, and M.F. Wang, Dual-grid FDTD scheme for fast simulation of surrounded antenna, IET Microwave Antenna Propag 3 (2007), 700–706.
13. R. Chantalat, C. Menudier, M. Thevenot, T. Monediere, E. Arnaud, and P. Dumon, Enhanced EBG resonator antenna as feed of a reflector antenna in the Ka-band, IEEE Antennas Wireless Propag Lett 7 (2008), 349–352.
14. A.A. Kishk, One-dimensional electromagnetic bandgap for directivity enhancement of waveguide antennas, Microwave Opt Technol Lett 47 (2005), 430–434.

INTEGRATION OF MONOPOLE SLOT AND MONOPOLE STRIP FOR INTERNAL WWAN HANDSET ANTENNA

Kin-Lu Wong and Po-Wei Lin
Department of Electrical Engineering, National Sun Yat-Sen University, Kaohsiung 804, Taiwan; Corresponding author: wongkl@ema.ee.nsysu.edu.tw

Received 13 September 2011

ABSTRACT: *A novel internal handset antenna formed by a monopole slot and a monopole strip for the wireless wide area network (WWAN) operation in the 824–960 and 1710–2170 MHz bands is presented. The monopole strip is disposed in the monopole slot, and both are embedded in the system ground plane of the handset with a small board space of 9 × 40 mm^2 at about the bottom edge of the circuit board. The monopole strip serves as a feed for the monopole slot and also functions as an efficient radiator. In the proposed design, the monopole slot generates a quarter-wavelength slot mode in the antenna's lower band, while the monopole strip contributes its quarter-wavelength mode in the antenna's upper band. By including a vertical strip that can be enclosed inside the handset casing or be a part of the bezel surrounding, the periphery of the handset casing and connected to the bottom edge of the system ground plane, the impedance matching of the excited slot mode can be greatly improved. In this case, the proposed antenna can provide two wide operating bands with good impedance matching to cover the pentaband WWAN operation. Detailed operating principle of the integrated monopole slot and monopole strip for the internal WWAN handset antenna is described. The proposed antenna is also fabricated and obtained results are presented and discussed.* © 2012 Wiley Periodicals, Inc. Microwave Opt Technol Lett 54:1718–1723, 2012; View this article online at wileyonlinelibrary.com. DOI 10.1002/mop.26870

Key words: *mobile antennas; handset antennas; monopole slot antennas; monopole; strip antennas; wireless wide area network antennas*

1. INTRODUCTION

The monopole slot is easy to fabricate and can operate at its quarter-wavelength mode as the lowest resonant mode [1–3], which makes it promising to achieve wideband operation with a small size for mobile handset applications. Recently, several printed monopole slot antennas covering the wireless wide area network (WWAN) operation in the mobile handset have been demonstrated [4–12]. These reported monopole slot handset antennas for the WWAN operation are mainly excited using a microstrip feedline, which is generally not an efficient radiator for frequencies in the desired operating bands of the antenna. As the monopole slot is a no-ground or clearance region embedded in the system circuit board of the handset, it is expected that a monopole strip disposed inside the monopole slot can be an efficient radiator and may contribute resonant modes in the desired operating bands of the antenna, if properly designed. In this case, the monopole strip not only can serve as a feed for the monopole slot but also can function like an efficient radiator to generate additional resonant modes in the antenna's desired operating bands. This can result in much wider operating bands achieved for the antenna. This design concept is implemented in this study.

In this article, we present a promising integration of the monopole slot and monopole strip for the WWAN operation in the mobile handset. The monopole strip is disposed in the monopole slot, and both are embedded in the system ground plane of the handset with a small board space of 9 × 40 mm^2 at about the bottom edge of the circuit board. The monopole strip in the proposed design comprises two branch strips and both can contribute their quarter-wavelength resonant modes to form into the antenna's upper band to cover the GSM1800/1900/UMTS operation in the 1710–2170 MHz band. That is, at higher frequencies, the monopole slot serves as a clearance region for the monopole strip to be an efficient radiator. On the other hand, at lower frequencies, the monopole strip becomes nonresonant and can serve as a feed for the monopole slot to generate its quarter-wavelength slot mode in the antenna's lower band. By further including a vertical strip that is connected to the bottom edge of the system ground plane, the impedance matching of the excited slot mode can be improved to cover the GSM850/900 operation in the 824–960 MHz band. Hence, the antenna can provide two wide operating bands to cover the pentaband WWAN operation. It should also be noted that in practical applications, the vertical strip can be enclosed inside the handset casing or placed on the

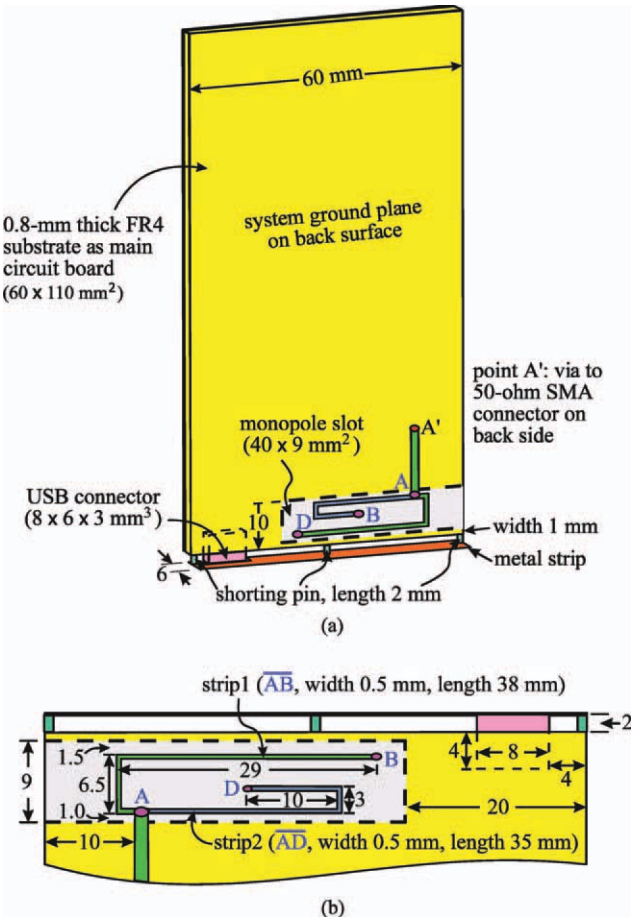

Figure 1 (a) Geometry of the integrated monopole slot and monopole strip for internal WWAN handset antenna. (b) Detailed dimensions of the proposed antenna. [Color figure can be viewed in the online issue, which is available at wileyonlinelibrary.com]

outer surface of the handset casing. In the latter case, the vertical strip can be a part of the bezel surrounding the periphery of the handset casing [13, 14]. Details of the operating principle of the proposed integration of the monopole slot and monopole strip for the WWAN operation in the mobile handset or smartphone are described. Results of the fabricated prototype of the proposed antenna are presented and discussed.

2. PROPOSED ANTENNA

Figure 1 shows the geometry of the integrated monopole slot and monopole strip for internal WWAN handset antenna. The monopole slot is a rectangular no-ground or clearance region of size 9×40 mm^2 embedded at near the bottom edge of the system ground plane of size 110×60 mm^2, which is printed on the back surface of a 0.8-mm thick FR4 substrate of relative permittivity 4.4 and loss tangent 0.024. The FR4 substrate can be treated as the main circuit board of a practical mobile handset or smartphone. The monopole slot is spaced with a narrow width of 1 mm to the bottom edge of the system ground plane. With the presence of the FR4 substrate that can decrease the resonant length of the slot mode, the selected size (length 40 mm and width 9 mm) of the monopole slot can generate a quarter-wavelength slot mode at about 900 MHz for the antenna's lower band to cover the GSM850/900 operation.

Inside the monopole slot, a monopole strip is printed on the front surface of the main circuit board. The monopole strip consists of two branch strips, strip1 and strip2, which are, respectively, of lengths 35 and 38 mm. The strip1 and strip2 can, respectively, contribute a resonant mode in the desired upper band. The two resonant modes are formed into a wide operating band to cover the GSM1800/1900/UMTS operation. Note that at higher frequencies, both the strip1 and strip2 are resonant elements and function as efficient radiators. Although at lower frequencies, the strip1 and strip2 are nonresonant elements and serve as exciters for the monopole slot to generate its quarter-wavelength slot mode.

Also, note that the monopole slot is disposed very close to the bottom edge of the system ground plane to achieve a compact size of the proposed antenna occupied in the main circuit board. For this consideration, the distance between the monopole slot and the bottom edge of the system ground plane is 1 mm only in this study, which, however, affects efficient excitation of the monopole slot. To alleviate this problem, a vertical strip of width 6 mm and length 60 mm is connected orthogonal to the bottom edge of the system ground plane as shown in the figure. The width of the vertical ground is 6 mm only and is less than the width of the modern handset on the market for the present. It is noted that the vertical strip can be placed inside the handset casing or on the outer surface of the handset casing. With the presence of the vertical strip, the narrow width between the monopole slot and the bottom edge of the system ground plane can be compensated, which can lead to better impedance matching for the excited slot mode at about 900 MHz such that the obtained bandwidth can cover the desired 824–960 MHz band.

It should be noted that at the ground plane nearby the monopole slot, associated electronic elements can be accommodated [11]. This is an attractive feature for the embedded monopole slot as an internal handset antenna. To demonstrate this feasibility, as shown in Figure 1, a micro-universal series bus (USB) connector [15–17] with a volume of $8 \times 6 \times 3$ mm^3 is mounted at the bottom edge of the system ground plane. The opening of the USB is placed at the vertical strip to serve as a data port with external devices. Based on the geometry shown in Figure 1, the proposed antenna was fabricated and tested. The photo of the fabricated antenna is shown in Figure 2, and the obtained results for the antenna with the USB connector mounted nearby are presented in Section 3 for discussion.

3. RESULTS OF FABRICATED ANTENNA

The measured return-loss results of the fabricated prototype of the proposed antenna are presented in Figure 3. The corresponding simulated return-loss results obtained using the three-dimensional (3D) full-wave electromagnetic field simulator high frequency structure simulator [18] are also shown for comparison. The measurement is seen to agree with the simulation. Based on the 3:1 VSWR or 6-dB return loss, which is widely used as the design specification of the internal WWAN mobile device antenna [19–21], two wide operating bands have been provided

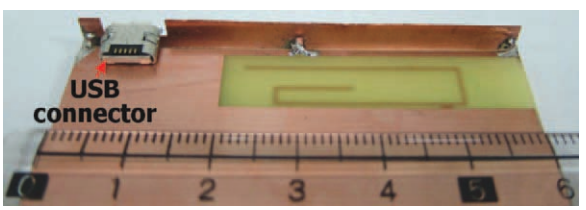

Figure 2 Photo of the fabricated antenna. [Color figure can be viewed in the online issue, which is available at wileyonlinelibrary.com]

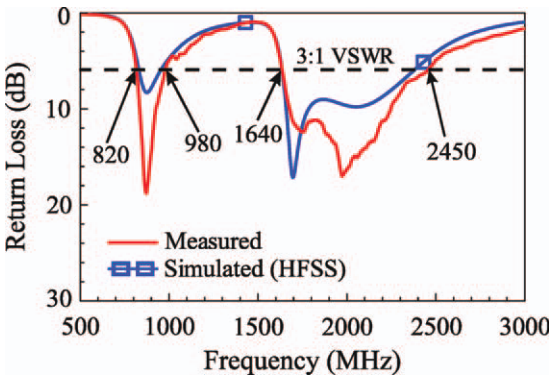

Figure 3 Measured and simulated return loss of the proposed antenna. [Color figure can be viewed in the online issue, which is available at wileyonlinelibrary.com]

by the antenna. The antenna's lower band is formed by a resonant mode at about 900 MHz and covers the GSM850/900 operation. The antenna's upper is formed by two resonant modes at about 1700 and 2000 MHz and covers the GSM1800/1900/UMTS operation. That is, pentaband WWAN operation is achieved by the proposed antenna.

To analyze the operating principle of the antenna, a comparison of the simulated return loss for the strip1 in the monopole strip only (Ant1), the strip1 and monopole slot only (Ant2), the strip1, monopole slot and vertical strip only (Ant3), and the proposed antenna is presented in Figure 4. Corresponding dimensions of the four antennas in this study are the same as shown in Figure 1. The structures of Ant1, Ant2, and Ant3 are also shown in the figure. For Ant1, it can be considered as a simple monopole strip antenna disposed on a no-ground region of 10 $\times$ 40 mm^2. In this case, there is no resonant mode occurred in the desired lower band at about 900 MHz. The resonant mode occurred at about 1500 MHz is a quarter-wavelength resonant mode contributed by the strip1. When a narrow ground strip of width 1 mm and length 40 mm is disposed at the bottom edge of the system ground plane to form an open slot of dimensions 9 $\times$ 40 mm^2, a monopole slot or quarter-wavelength slot antenna can be created. It can be seen that a resonant mode at about 900 MHz is generated, which is contributed by the monopole slot. Further, probably owing to added narrow ground strip that induces some coupling with the strip1, the excited resonant mode contributed by the strip1 is shifted to higher frequencies at about 2000 MHz.

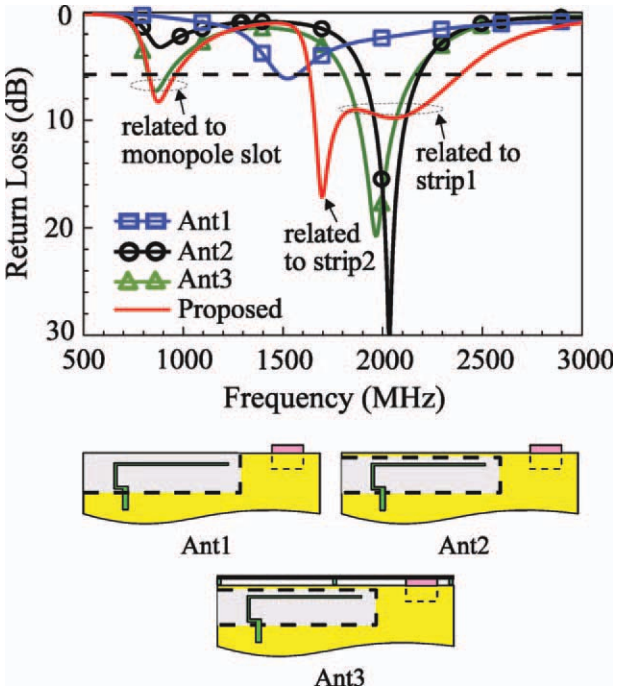

Figure 4 Simulated return loss for the strip1 of the monopole strip only (Ant1), the strip1 and monopole slot only (Ant2), the strip1, monopole slot, and vertical strip only (Ant3), and the proposed antenna. [Color figure can be viewed in the online issue, which is available at wileyonlinelibrary.com]

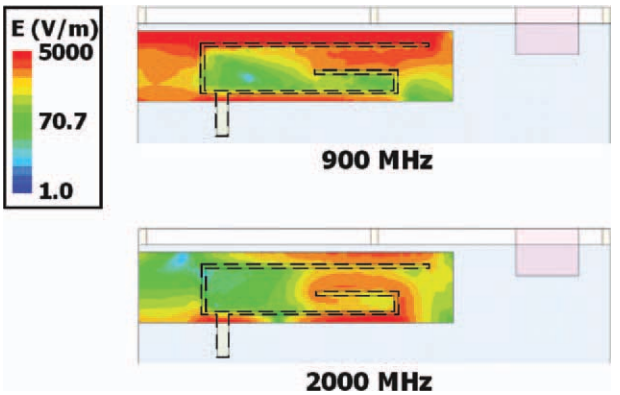

Figure 5 Simulated electric-field distribution excited in the open slot region of the proposed antenna at 900 and 2000 MHz. [Color figure can be viewed in the online issue, which is available at wileyonlinelibrary.com]

When the vertical strip is further added to Ant2 (i.e., Ant3 is formed), the impedance matching of the exited slot resonant mode contributed by the monopole slot is improved. Finally, to achieve a wide upper band for the antenna, the strip2 is added to form a two-branch monopole strip in the proposed antenna. In this case, an additional resonant mode contributed by the strip2 is seen to occur at about 1700 MHz, which combines the resonant mode at about 2000 MHz contributed by the strip1 to result in a wide operating band to cover the 1710–2170 MHz band. Some improvements in the impedance matching of the resonant mode at about 900 MHz are also seen.

The simulated electric-field distribution excited in the open slot region of the proposed antenna at 900 and 2000 MHz is also presented in Figure 5 for comparison. It can be seen that at 900 MHz, strong electric fields at the open end of the slot are excited, which is in general decreases to be null at the closed end of the slot. This behavior is similar to the observations of the monopole slot excitation discussed in Ref. 22 and can confirm that the quarter-wavelength slot mode is excited at about 900 MHz for the antenna. On the other hand, at 2000 MHz, the electric-field distribution inside the open slot region is relatively very weak, except around the open ends of the strip1 and strip2. This behavior agrees with the results shown in Figure 4, in which it shows that the resonant modes at around 2000 MHz are not contributed by the open slot as a radiator.

Results of the simulated return loss as a function of the monopole slot length L are also presented in Figure 6. Results for the slot length L varied from 40 to 46 mm are shown. Other dimensions of the antenna are the same as shown in Figure 1. It is seen that the excited resonant mode in the antenna's lower band is shifted to lower frequencies with an increase in the

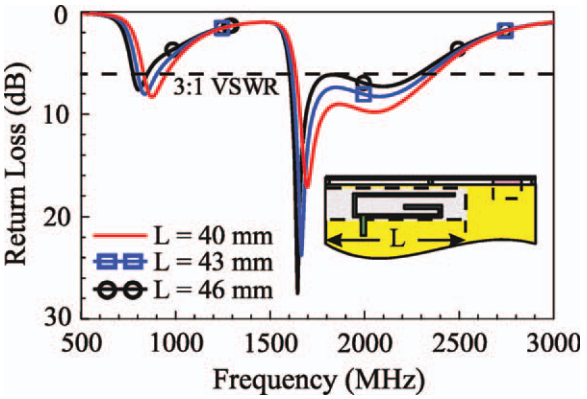

Figure 6 Simulated return loss as a function of the monopole slot length *L*. Other dimensions are the same as shown in Figure 1. [Color figure can be viewed in the online issue, which is available at wileyonlinelibrary.com]

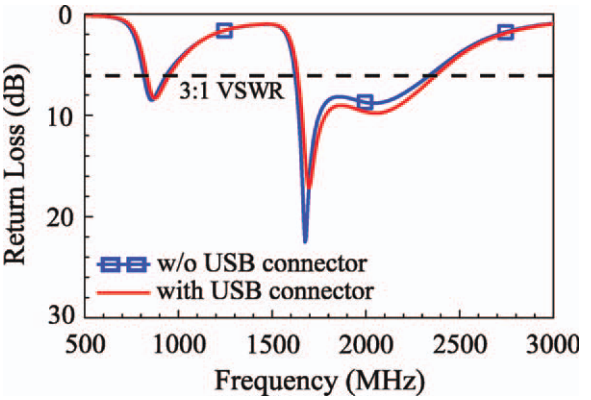

Figure 8 Simulated return loss for the proposed antenna with and without the USB connector. Other dimensions are the same as shown in Figure 1. [Color figure can be viewed in the online issue, which is available at wileyonlinelibrary.com]

length *L*. This behavior is reasonable as the excited resonant mode at about 900 MHz is mainly contributed by the monopole slot. Also, it is seen that there are some variations on the impedance matching of the two resonant modes contributed by the strip1 and strip2 in the antenna's upper band. This is largely because the slot region serves as a clearance or no-ground region for the strip1 and strip2 to function efficient radiators; hence, the variations in the dimensions of the slot region will also cause some effects on the resonant modes generated by the strip1 and strip2.

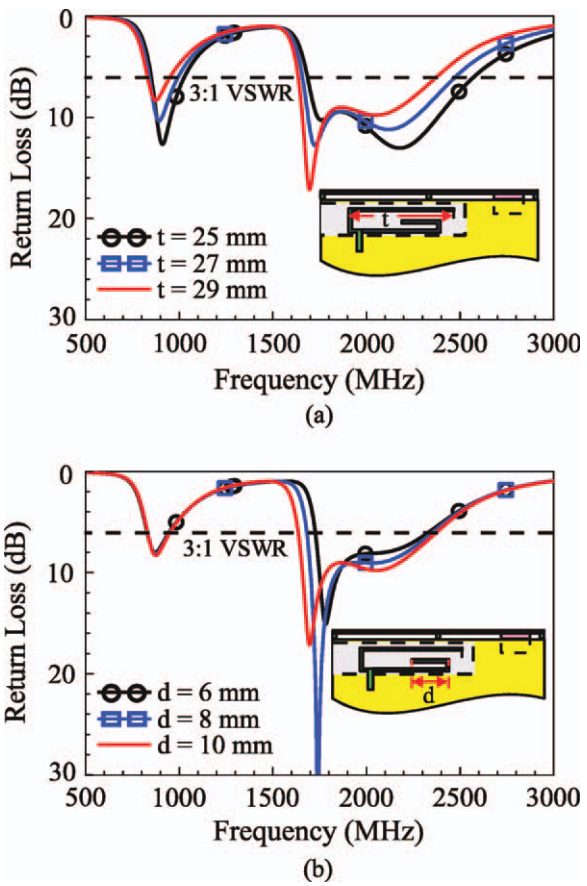

Figure 7 Simulated return loss as a function of (a) the length *t* in the strip1 and (b) length *d* in the strip2. Other dimensions are the same as shown in Figure 1. [Color figure can be viewed in the online issue, which is available at wileyonlinelibrary.com]

Effects of the length variations in the strip1 and strip2 on the antenna performances are also analyzed. Results of the simulated return loss for the length *t* in the strip1 varied from 25 to 29 mm are shown in Figure 7(a) while those for the length *d* in the strip2 varied from 6 to 10 mm are shown in Figure 7(b). Other dimensions of the antenna are the same as shown in Figure 1. In Figure 7(b), the resonant mode at about 1700 MHz is seen to be shifted to higher frequencies with a decrease in the length *d*. This behavior agrees with the observation in Figure 4 that the resonant mode at about 1700 MHz is contributed by the strip2 and it can be mainly controlled by the strip2. Similarly, in Figure 7(a), it is seen that the second mode in the upper band is shifted to higher frequencies with a decrease in the length *t*, indicating that it can be controlled by the strip1. This also causes some impedance variations for the first mode in the upper band. In addition, some effects on the resonant mode contributed by the monopole slot at about 900 MHz are also seen. This is largely owing to the coupling effects between the strip1 and the narrow ground strip at the bottom edge of the system ground plane, which has been observed to cause some variations in the resonant mode generated by the strip1 in Figure 4 (see the results of Ant1 vs. Ant2).

Figure 8 shows the simulated return loss for the proposed antenna with and without the USB connector. Small effects on the impedance matching of the antenna are seen. This behavior suggests that the portion of the system ground portion nearby the antenna can be reclaimed to accommodate associated electronic elements, which is attractive for compact integration of the proposed antenna in the mobile handset.

The radiation characteristics measured in a far-field anechoic chamber are also studied. Figure 9 shows the measured antenna efficiency of the proposed antenna that includes the mismatching loss. The antenna efficiency is varied, respectively, from about 58 to 85% and 53 to 80% over the lower and upper bands, which is acceptable for practical handset applications [23]. The measured 3D total-power radiation patterns of the proposed antenna are plotted in Figure 10. Results for five testing frequencies are presented. At each frequency, the full 3D patterns seeing in the *x* direction and the half 3D patterns with the cross-sectional cut at the *y*–*z* plane are shown. Dipole-like radiation patterns are seen at 859 and 925 MHz, which are similar to the observations for many internal WWAN/LTE handset antennas

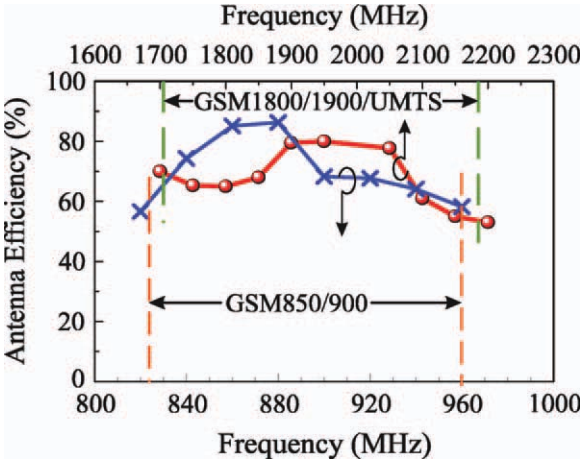

Figure 9 Measured antenna efficiency (mismatching loss included) of the proposed antenna. [Color figure can be viewed in the online issue, which is available at wileyonlinelibrary.com]

[24–27]. At higher frequencies, stronger radiation in the upper ($+z$) half-plane than in the lower ($-z$) half-plane is seen. This behavior is largely because the resonant modes in the antenna's upper band are quarter-wavelength resonant modes contributed by the strip1 and strip2, and the monopole strips usually excite strong surface currents on the system ground plane as well. This leads to stronger radiation seen in the upper ($+z$) half-plane.

Figure 11 shows the SAR simulation models and the simulated SAR values [28, 29] for the proposed antenna. The SAR results for three conditions of the head only, the hand only, and the head and hand are studied. The simulation models are provided by the SPEAG simulation software SEMCAD X version 14 [30]. The handset casing, which is a virtual casing in this study, is attached to right cheek of the phantom head with no tilt, and the distance between the ear and the system ground plane is 4.2 mm. The grip of the phantom hand holding the handset is shown in the figure, and the maximum distance between the palm and the system ground plane is set to 29.2 mm. The SAR results for 1-g tissue are shown in the table in the figure, based on the input power of 24 dBm for the GSM850/900 operation at 859 and 925 MHz and 21 dBm for the GSM1800/1900 operation at 1795 and 1920 MHz and the UMTS operation at 2045 MHz.. The return loss for the three different conditions at each testing frequency is also given in the table. For the head only condition, the 1-g SAR values are less than the 1.6 W/kg [28], the allowed maximum value for practical applications. For the hand only condition, the SAR values are in general larger than those for the head only condition. This may be related to the grip position of the hand phantom in the study, in which the little figure of the phantom hand is very close to the open end of the monopole slot. For the head and hand condition, note that the SAR values occurred at the phantom head are also shown in the parentheses. At 859 MHz, the SAR value of 1.83 W/kg occurs at the phantom hand, so are those at other testing frequencies for the head and hand condition. When only the SAR values occurred at the phantom head

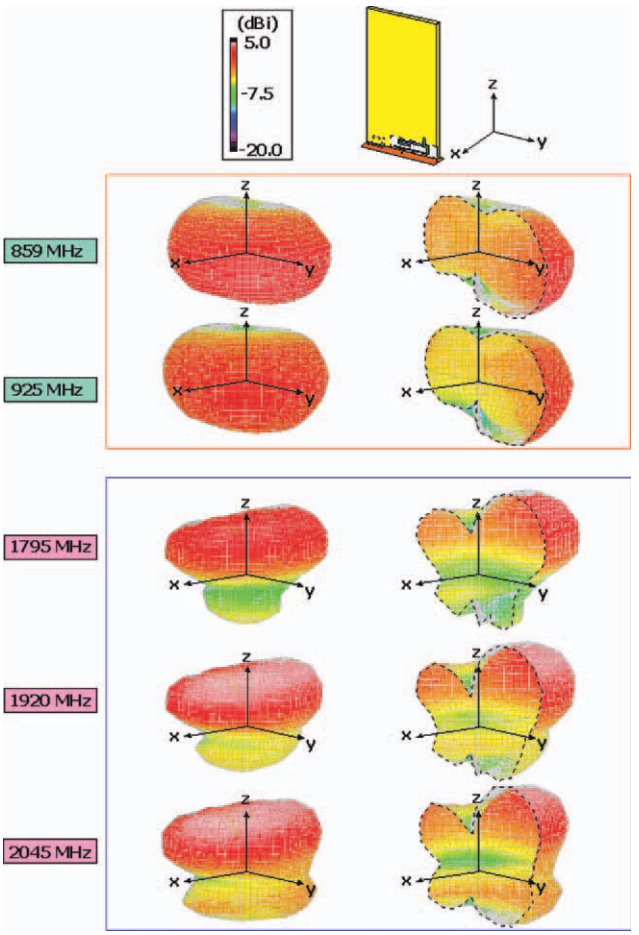

Figure 10 Measured 3D total-power radiation patterns of the proposed antenna. [Color figure can be viewed in the online issue, which is available at wileyonlinelibrary.com]

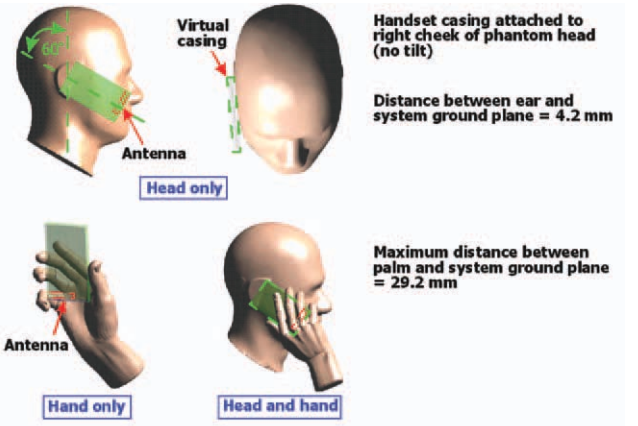

Frequency (MHz)		859	925	1795	1920	2045
SAR (W/kg)	head only	1.47	1.22	0.80	0.71	0.70
	hand only	1.67	1.19	0.93	0.91	0.96
	head and hand	1.83 (1.40)*	1.28 (1.27)*	0.72 (0.57)*	0.77 (0.65)*	0.82 (0.74)*
Return loss (dB)	head only	9.8	6.3	18.7	17.0	19.5
	hand only	14.3	8.2	18.3	16.5	15.1
	head and hand	14.3	7.4	18.2	20.0	17.0

( )*: SAR Value occurred at the head for the case of head and hand

Figure 11 SAR simulation models and the simulated 1-g SAR values for the proposed antenna. [Color figure can be viewed in the online issue, which is available at wileyonlinelibrary.com]

are considered, the proposed antenna also meets the SAR regulation for the head and hand condition.

4. CONCLUSIONS

An integrated monopole slot and monopole strip for pentaband WWAN operation in the mobile handset has been proposed, fabricated, and tested. The antenna requires a small board space of 9×40 mm^2 on the main circuit board of the handset and can be embedded very close to the bottom edge of the circuit board. In the proposed antenna, the monopole slot is excited to contribute a resonant mode for the antenna's lower band, while the monopole strip formed by the strip1 and strip2 and embedded inside the monopole slot also contributes resonant modes for the antenna's upper band. Good radiation characteristics of the proposed antenna over the operating bands have been observed. The simulated 1-g SAR values of the antenna for three conditions of the head only, the hand only, and the head and hand have been analyzed. The obtained results indicate that the antenna is promising to meet the SAR regulation, especially when only the SAR values occurred at the phantom head are considered.

REFERENCES

1. H. Wang, M. Zheng, and S.Q. Zhang, Monopole slot antenna, US Patent No. 6618020 B2, Sep. 9, 2003.
2. S.K. Sharma, L. Shafai, and N. Jacob, Investigation of wide-band microstrip slot antenna, IEEE Trans Antennas Propag 52 (2004), 865–872.
3. A.P. Zhao and J. Rohola, Quarter-wavelength wideband slot antenna for 3–5 GHz mobile applications, IEEE Antennas Wireless Propag Lett 4 (2005), 421–424.
4. P. Lindberg, E. Ojefors, and A. Rydberg, Wideband slot antenna for low-profile hand-held terminal applications, In: Proc 36th European Microwave Conference, Manchester, UK, 2006, pp. 1798–1701.
5. C.I. Lin and K.L. Wong, Printed monopole slot antenna for internal multiband mobile phone antenna, IEEE Trans Antennas Propag 55 (2007), 3690–3697.
6. F.H. Chu and K.L. Wong, Simple folded monopole slot antenna for penta-band clamshell mobile phone application, IEEE Trans Antennas Propag 57 (2009), 3680–3684.
7. C.H. Wu and K.L. Wong, Hexa-band internal printed slot antenna for mobile phone application, Microwave Opt Technol Lett 50 (2008), 35–38.
8. C.H. Wu and K.L. Wong, Internal hybrid loop/monopole slot antenna for quad-band operation in the mobile phone, Microwave Opt Technol Lett 50 (2008), 795–801.
9. C.H. Chang and K.L. Wong, Internal multiband surface-mount monopole slot chip antenna for mobile phone application, Microwave Opt Technol Lett 50 (2008), 1273–1279.
10. C.I. Lin and K.L. Wong, Printed monopole slot antenna for penta-band operation in the folder-type mobile phone, Microwave Opt Technol Lett 50 (2008), 2237–2241.
11. K.L. Wong, P.W. Lin, and C.H. Chang, Simple printed monopole slot antenna for penta-band WWAN operation in the mobile handset, Microwave Opt Technol Lett 53 (2011), 1399–1404.
12. K.L. Wong and P.W. Lin, Surface-mount WWAN monopole slot antenna for mobile handset, Microwave Opt Technol Lett 53 (2011), 1890–1896.
13. R.J. Hill, R.W. Schlub, and R. Caballer, Antennas for handheld electronic devices with conductive bezels, US Patent No. 7843396 B2, Nov. 30, 2010.
14. M. Pascolini, R.J. Hill, J. Zavala, N. Jin, Q. Li, R.W. Schlub, and R. Caballero, Bezel gap antennas, US Patent Publication No. 2011/0136447 A1, Jun. 9, 2011.
15. Wikipedia, the free encyclopedia: Universal Serial Bus (USB), Available at: http://en.wikipedia.org/wiki/Universal_Serial_Bus.
16. K.L. Wong and C.H. Chang, On-board small-size printed monopole antenna integrated with USB connector for penta-band WWAN mobile phone, Microwave Opt Technol Lett 52 (2010), 2523–2527.
17. K.L. Wong, W.Y. Chen, and T.W. Kang, On-board printed coupled-fed loop antenna in close proximity to the surrounding ground plane for penta-band WWAN mobile phone, IEEE Trans Antennas Propag 59 (2011), 751–757.
18. Ansoft Corporation HFSS, Available at: http://www.ansoft.com/products/hf/hfss/.
19. H.W. Hsieh, Y.C. Lee, K.K. Tiong, and J.S. Sun, Design of a multiband antenna for mobile handset operations, IEEE Antennas Wireless Propag Lett 8 (2009), 200–203.
20. J.H. Kim, W.W. Cho, and W.S. Park, A small printed dual-band antenna for mobile handsets, Microwave Opt Technol Lett 51 (2009), 1699–1702.
21. C.L. Liu, Y.F. Lin, C.M. Liang, S.C. Pan, and H.M. Chen, Miniature internal penta-band monopole antenna for mobile phones, IEEE Trans Antennas Propag 58 (2010), 1008–1011.
22. K.L. Wong and F.H. Chu, Internal planar WWAN laptop computer antenna using monopole slot elements, Microwave Opt Technol Lett 51 (2009), 1274–1279.
23. A. Andujar, J. Anguera, and C. Puente, Ground plane boosters as a compact antenna technology for wireless handheld devices, IEEE Trans Antennas Propag 59 (2011), 1668–1677.
24. K.L. Wong, M.F. Tu, C.Y. Wu, and W.Y. Li, On-board 7-band WWAN/LTE antenna with small size and compact integration with nearby ground plane in the mobile phone, Microwave Opt Technol Lett 52 (2010), 2847–2853.
25. F.H. Chu and K.L. Wong, Simple planar printed strip monopole with a closely-coupled parasitic shorted strip for eight-band LTE/GSM/UMTS mobile phone, IEEE Trans Antennas Propag 58 (2010), 3426–3431.
26. Y.W. Chi and K.L. Wong, Internal compact dual-band printed loop antenna for mobile phone application, IEEE Trans Antennas Propag 55 (2007), 1457–1462.
27. K.L. Wong and S.C. Chen, Printed single-strip monopole using a chip inductor for penta-band WWAN operation in the mobile phone, IEEE Trans Antennas Propagat 58 (2010), 1011–1014.
28. American National Standards Institute (ANSI), Safety levels with respect to human exposure to radio-frequency electromagnetic field, 3 kHz to 300 GHz, ANSI/IEEE standard C95.1, Apr. 1999.
29. IEC 62209–1, Human exposure to radio frequency fields from hand-held and body-mounted wireless communication devices—Human models, instrumentation, and procedures—Part 1: Procedure to determine the specific absorption rate (SAR) for hand-held devices used in close proximity to the ear (frequency range of 300 MHz to 3 GHz), Feb. 2005.
30. Schmid & Partner Engineering AG (SPEAG), Available at: http://www.semcad.com, SEMCAD.

MICROSTRIP LOWPASS FILTER BASED ON SPLIT RING AND COMPLEMENTARY SPLIT RING RESONATORS

Yang Yang, Xi Zhu, and Nemai C. Karmakar
Department of Electrical and Computer Systems Engineering, Monash University, Building 72, Clayton Campus, Melbourne, VIC 3800, Australia; Corresponding author: yang.yang@monash.edu

Received 17 September 2011

ABSTRACT: *A novel split ring and complementary split ring resonator is proposed in this letter. The proposed resonator can generate two notches without increasing the physical size. A microstrip lowpass filter (LPF) is designed based on the proposed resonator. The cutoff frequency of the designed LPF is 3.7 GHz and the stopband with an*